Novel insights from point-dendrometers in an urban setting: linking environmental variation to fluctuations in stem radius.

Kevin L. Griffin, PhD[1,2,3,*]
Thomas G. Harris [4]
Sarah Bruner, M.A. [1]
Patrick McKenzie, M.A. [1]
Jeremy Hise, B.A. [1,5]

[1]Department of Ecology, Evolution and Environmental Biology, Columbia University, New York, NY 10027, USA

[2]Department of Earth and Environmental Sciences, Columbia University, Palisades, NY 10964, USA

[3]Lamont-Doherty Earth Observatory, Columbia University, Palisades, NY 10964, USA

[4] Mc, New York, NY 10025, USA

[5] Hise Scientific Instrumentation, LLC., 378 Route 202 Suite 2A Somers, New York 10589 USA

*** Corresponding Author:** Kevin L. Griffin, Lamont-Doherty Earth Observatory of Columbia University, 61 Route 9W, Palisades NY 10964. (845)422-1364. griff@LDEO.columbia.edu

Abstract:

Background: The unique environment of urban/suburban areas affects tree growth in surprising and currently unrecognized ways. Real-time monitoring of tree growth could provide novel information about these trees and the myriad ecosystem services they provide.

Methods: Internet enabled, high-resolution point dendrometers were installed on four trees in Southampton, NY. The instruments, along with a weather station, streamed data to a project web page that was updated once an hour. (https://ecosensornetwork.com).

Results: Radial growth of spruce began April 14 after the accumulation of 69.7 °C growing degrees days and ended September 7th. Cedar growth began later (4/26), after the accumulation of 160.6 °C and ended later (11/3). During our observations, these three modest suburban trees sequestered 108.3 kg of CO_2. Growth took place primarily at night and was best predicted by a combination of air temperature, soil moisture, VPD and interaction terms.

Conclusions: This project's two-year time series provided insights into the growth of trees in a residential area. Linking tree growth to fluctuations in environmental conditions facilitates the development of a mechanistic predictive understanding useful for ecosystem management and growth forecasting across future altering climates. Live-streaming tree growth data enables a deeper appreciation of the biological activity of trees and the ecosystem services they provide in urban environments and thus can be a powerful tool connecting urban social and ecological systems.

Keywords: Carbon sequestration, Climate, *Cryptomeria japonica, Picea glauca,* Tree Growth

Introduction:

The biogeophysical environment of urban areas is substantially different from that of rural ones. Humans are altering the hydrologic cycle of exurban watersheds, both by importing vast amounts of fresh water (Booth & Bledsoe, 2009) and through the widespread use of impervious materials that modify the local water balance by decreasing groundwater recharge and increasing surface water runoff (Haase, 2009; Walsh et al., 2012). Urban centers modify the local climate by releasing sensible heat from artificial surfaces warmed during the day (Weng, 2003; Hamin & Gurran, 2009; McGeehin & Mirabelli, 2001). Airborne particulates in urban areas can create rain-inducing condensation nuclei that result in increased precipitation in, and downwind of, cities (Shepherd et al., 2002). Urban air itself contains increased concentrations of pollutants such as CO_2, nitrogen oxides, sulfur oxides, ozone and other volatile organic compounds (Chameides et al., 1992; Idso et al., 1998; Lovett et al., 2000; Nowak et al., 2006; Calfapietra et al., 2013). Urban soils often contain elevated levels of heavy metals (Bernhardt et al., 2008; Kaushal & Belt, 2012; Sonti et al., 2019). Furthermore, changes in rates of litter decomposition (Carreiro et al., 1999), mineralization and nitrification (Zhu & Carreiro, 2004), and shifts in soil faunal communities (Steinberg et al., 1997) affect local biogeochemical cycles of essential nutrients. Finally, increased abundance of exotic species in urban areas is contributing to significant changes in species composition in urban ecosystems (Rudnicky & McDonnell, 1989). Understanding how these biogeophysical conditions and changes impact urban ecosystem services and the communities that depend on them is of critical importance.

Trees and tree growth provide a multitude of important benefits for urban ecosystems and their residents that can help mitigate many of the negative changes caused by urbanization (Figure 1). For example, among the many commonly recognized ecosystem services (e.g. Nitoslawski et al., 2019) provided by urban forests are: carbon sequestration and storage (Nowak & Crane, 2002; Pataki et al., 2006; Edmondson et al., 2012); stormwater and flood water management (Denman et al., 2016); improved nutrient cycling (Livesley et al., 2016); local cooling (Norton et al., 2015; Solecki et al., 2005); reductions of air pollution (Dochinger, 1980; Nowak et al., 2006; Abhijith et al., 2017); and increases in biodiversity (Ikin et al., 2013). At the same time, tree function, e.g. growth, reproduction, fitness and survival, are all heavily influenced by these same environmental factors. In this way, trees play a key role in urban ecosystems both affecting and being affected by the biogeophysical environment and thus understanding the physiological underpinnings of tree growth in urban forests is essential.

Traditionally tree growth is measured infrequently at low resolution. For example, foresters use methods of the USDA - Forest Service's Forest Inventory Analysis program (https://www.fia.fs.fed.us) such as recording diameter at breast height (DBH = 1.37m from the ground) to calculate basal area. Assessed yearly, these can provide growth rates; tree cores yield similar information and can be taken at a single time point, but require additional analysis (Sonti et al., 2019). Street tree surveys of size and health are part of many urban parks programs (Nowak et al., 2018) and aerial photographs (Spurr & Brown Jr, 1946) can provide useful insights as to quality and distribution of urban greenery. More recently, technological solutions such as aerial LiDAR (Alonzo et al., 2014), drones (Elliott, 2016), and satellites (Palomino et al., 2017; reviewed in Nitoslawski et al., 2019) show great potential to add in the understanding of tree growth in urban environments. All of these approaches, however, require repeat observations which can be expensive and/or infrequent. As a result of the limited spatial and temporal scales of the tree growth products typically obtained, our understanding of the links between the biogeophysical environment and the physiological underpinnings of tree growth in urban forests is similarly limited.

Dendrometers provide an alternative method of monitoring radial growth of trees and could provide much needed high-resolution data in urban ecosystems. When permanently mounted to the non-living sapwood of the tree, these highly responsive tree growth sensors can record when new cells are produced by the vascular cambium and/or the hydration of the immature xylem, cambium, phloem, or bark (Zweifel et al., 2014). Not only can these instruments provide detailed records of radial stem growth and water use (Steppe et al., 2006; Zweifel et al., 2006), when used in urban settings the instruments are easily connected to the internet and can

stream data live in real or near-real time. The result is a time series of stem radius that can be used for research, education and outreach and provides a much-needed link between growth and the environment.

In this study, we installed four dendrometers in a suburban backyard along with a research grade weather station to study the short time-scale interactions between tree growth and climatic conditions in urban environments. A two-year time series reveals unique insights into tree function and links to local weather and climate. We use this time series to model tree growth and total water deficit (TWD or water deficit-induced shrinking and swelling of the stem) as in Zweifel et al. (2016). We define statistical relationships between growth, the phenology of growth, and TWD, and light, temperature, soil moisture and growing degree days. In addition to the lessons learned we evaluate the usefulness of this monitoring approach and discuss the research, education and outreach potential of an expanded dendrometer network in urban forests.

Methods:

Location and Plant Material:

Four adjacent ornamental trees growing in a backyard tree in Southampton, NY (USA), were used for this study, two white spruce (*Picea glauca* (Moench) Voss) and two Japanese cedar (*Cryptomeria japonica* (L. f.) D. Don). The experiment was established in June of 2018. The native soils of this location are of the Bridgehampton silt loam association (NRCS, 2009) and are both well-drained and inherently low in mineral nutrition. However, significant soil improvement, modification and the addition of organic materials and fertilizers has taken place. The study area is irrigated and thus the study trees rarely experience prolonged water limitation. The climate of Southampton is maritime and strongly seasonal with historical July (the warmest month) minimum and maximum temperatures averaging 18 and 27 °C respectively and historical January (the coldest month) minimum and maximum temperatures averaging -4.4 and 3.9 °C respectively (https://prism.oregonstate.edu/explorer/). Rainfall is nearly constant throughout the year averaging 106.43 mm $month^{-1}$ and totaling 1.28 m yr^{-1}. Growing degree days were also calculated as the accumulated average temperatures above 5 °C following the coldest day of the year

Diameter Growth and Environmental Monitoring:

A time series of tree diameter was continuously recorded by a point dendrometer (Hise Scientific Instrumentation, Somers, New York USA). The dendrometer is attached to the stem of the tree using a mounting bracket that maintains the potentiometer in a fixed position relative to the non-living xylem with a stainless steel 6.35 mm diameter rod, inserted approximately one cm into the stem. All dendrometers were placed on the north side of the tree (to minimize exposure to direct solar radiation) at a height of 1.37 m from the ground surface. Dendrometers were installed on top of the thin bark (after carefully removing any loose bark with a small rasp, while avoiding damage to the living tissues), and thus all processes causing the changes in stem diameter below the location of the sensor were recorded. These may include: bark swelling and shrinking, cambial activity, changes in phloem, xylogenesis and stem hydraulics. Every five minutes the average position of the sensor was recorded (EM50G, METER Group Inc, Pullman, WA USA). Each potentiometer was independently calibrated at the time of installation and output is considered linear over the very small annual change (<3 mm) with the effect of temperature on the measurement being minimal (Eitel et al., 2020). Each sensor's initial voltage was related to the measured stem diameter at DBH, which allowed us to continuously calculate the stem radius.

Local environmental conditions at the experimental site were monitored throughout the experiment using a digital weather station (ATMOS 41, METER Group Inc, Pullman, WA USA). This station measures: Solar radiation, precipitation, air temperature, barometric pressure, vapor pressure, relative humidity, wind speed, wind direction, maximum wind gust, lightning strikes, lightning distance and tilt. In addition, soil moisture, soil temperature and conductivity were measured in a single location, at a depth of 10 cm, approximately 2.5m from Spruce 2 and Cedar 1 (TEROS 12, METER Group Inc, Pullman, WA USA) All environmental, soil, and growth data were recorded as five min averages with a single data logger (see above) and each hour these data were automatically uploaded to the Zentra Cloud (METER Group Inc, Pullman, WA USA). From here the data were

transferred to the Eco Sensor Network (ESN, Hise Scientific Instrumentation, Somers, New York USA) where the data are publicly available in near real time (https://ecosensornetwork.com).

To convert changes in stem radius to biomass, biomass increments and rates of aboveground carbon sequestration, standard geometric relationships were assumed so that allometric biomass equations could be applied to the calculated DBH (stem diameter in cm measured 1.37m from the ground). White spruce aboveground biomass (kg) was calculated as $0.0777*DBH^{2.4720}$ (Harding & Grigal, 1985). No allometric equation specific to *Cryptomeria japonica* was found so biomass was calculated as exp(-2.0336 + 2.2592*ln(DBH)), a general equation for cedar & larch (Jenkins et al., 2003). Root mass for both species was conservatively estimated at 30% of the aboveground mass, based on the results of white spruce total biomass harvest performed by Ker and van Raalte (1981). Carbon sequestration was calculated as the increment in dry mass accumulation, assuming the carbon content of woody biomass is 50% (Thomas & Martin, 2012). By extension CO_2 can then be calculated based on the atomic ratio of one carbon atom to two oxygen atoms in each molecule of CO_2 with atomic weights of 12 and 16 grams per mole (a total of 44 grams per mole of CO_2), thus the weight of carbon was multiplied by 3.67.

Statistical analysis:
R version 3.4.4 was used for all statistical analyses (R Development Core Team, 2006). Due to low battery levels, not every 5-minute interval was recorded during a 24-hour period. Days missing more than 75% of their data were removed. Data were further cleaned manually by removing dramatic outlying points prior to further analysis.

Growth Models
Growing seasons for each tree were determined by using a piecewise regression which iteratively searched for a breakpoint by minimizing the mean squared error of the segments (Crawley, 2012). This was done separately for each tree and for the beginning and end of each season.

To estimate growth periods at the diurnal timescale, we used three different models: a smoothing spline (SS, Herrmann et al., 2016), a zero-growth model (ZG, Zweifel et al., 2016), and a Hidden-Markov Model (HMM, Eddy, 2004). The SS was fit to each tree's dendrometer readings with the degrees of freedom equal to the number of days in the interval to capture the daily trends of growth (Herrmann et al., 2016). In order to find the derivative of the residual of the SS, we approximated the average SS residual data from the six-week period using a sinusoidal function. We then were able to differentiate the sinusoidal function. For ZG, growth began when the current dendrometer exceeded the last maximum and ended at the first decreasing reading.

Within each growing season, we used an HMM to assign each time point to one of two latent variable states: "growth" or "deficit" (Durbin et al., 1998; Eddy, 2004). The model was trained using emitted states of the Zweifel et al. (2016) zero-growth model (ZG). The emitted states describe whether each time point is reaching an all-time high trunk diameter. We used the Baum-Welch algorithm to infer model parameters from the full data for each tree, and we used the Viterbi algorithm to infer the most likely state of the latent variable at each point (Durbin et al., 1998). All HMM code was implemented using the package `HMM` in R (R Development Core Team, 2006; Himmelmann, 2010).

For downstream statistics, we isolated the HMM-identified "growth" periods that overlapped with more than two data points. From these growth periods we derived our response variables and our predictors. The response variables are 1) the net change in the zero-growth model through the growth interval (y_{end}-y_{start}) and 2) the value from (1) divided by the duration of the growth interval. The value of (2) corresponds to the slope of a line passing through the zero growth model values at the beginning and end of the growth interval. The predictors are environmental variables. We calculated their values using the mean through the growth interval.

Linear models:
As most of growth occurs at night, we conducted a multiple regression analysis on the HMM-identified growth periods when solar radiation was equal to zero. The models were applied separately to each tree and to the "total growth" and "slope" response variables for each interval. During each interval, we used the mean of each environmental factor and their interactions as the explanatory variables.

Inference:
Conditional inference trees (CITs)
We performed a conditional inference tree (CIT) analysis using the *partykit* package in R (Hothorn & Zeileis, 2015). Conditional inference trees are a type of decision tree, a model class that recursively partitions the response variable by repeatedly splitting the data at a value of specific predictors. Conditional inference trees avoid biases associated with other decision tree variants by first using permutation tests for significance to identify the variable to split (selecting based on the minimum p-values) and then selecting the split point using a two-sample statistic. In addition to avoiding biases associated with related methods (e.g. CART), this method has an established stopping criterion and variable selection procedure, improving interpretability of results (Hothorn et al., 2006; Sarda-Espinosa et al., 2017).

The CITs were fit on the HMM-identified "growth" periods for each tree, with response variables being the "total growth" and "slope" metrics defined in the previous section. The predictors were the mean values of the environmental variables through each interval.

Results:
Micrometeorological conditions:
Air temperature during our experiment varied from a low of 4.8°C (5/1/19) to a high of 32.0 °C (7/14/19), with a mean temperature of 19.37± 5.18 °C (Figure 2). Daytime temperatures were on average 3 °C degrees warmer than nighttime temperatures, 20.581 ± 5.15 and 17.97±4.84 respectively, during the experimental period. Soil temperatures varied between 24.4 (8/9/18) and 8.7 with a mean of 18.3 ± 4.26 °C (Figure 2). Total precipitation was 1011.59 mm, coming in 28 discrete storm events averaging 18.097 mm (Figure 2). The combination of rain and irrigation resulted in a mean volumetric soil water content of 0.38±.026 m^3 m^{-3}. The wind was primarily onshore, coming from the south/southwest (201 °) (data not shown). The total solar energy received during the experimental period was 8.9 MW m^{-2}, with a daily average of 816.6 W m^{-2} d^{-1}.

Stem diameter:
The initial diameters of the four trees were 11.5 and 14.0 cm for the two spruce trees and 16.7 and 16.1 for the two cedars (Table 1). Over the two-year duration of the experiment, three of these trees grew by an average of 11% reaching final diameters of 13.4, 15.9 & 17.34 (Figure 3). The period of rapid diameter growth began on 4/14 ± 10 days, and ended on 9/07 ± 10 days (spruce) and began on 4/26, and ended on 11/3 ± 5 days (cedar, dotted vertical lines on Figure 3). Note a small portion of the 2018 early season growth may have occurred prior to the start of this experiment and thus be absent record and the two white spruce trees grew enough to saturate the dendrometer signal by end of the 2019 growing season (Figure 3a & b). The cedar showed slow but continuous growth during the winter season when the spruce trees were clearly not growing and, in some cases, showed a decrease in stem diameter due to winter dehydration (Figure 3c). The basal area increments added to these trees were 37.2, 29.0 and 7.8 cm^2 (for Spruce 1, Spruce 2 and Cedar 1 respectively) during the experiment. The fourth tree, Cedar 2, did not grow significantly during the first growing season and thus was excluded from further analysis.

Partitioning to growth and hydrologic responses:
Figure 4 displays two six-day periods: July 14th - 20th represents a period of rapid stem growth (Figure 4a, c, e & g); June 12th - 18th a period of limited growth but large hydrologic fluctuations (Figure 4b, d, f & h). Figure 4a & c compare the measured SR with the SS. The SS displays the overall growth trend during the two periods, upward trending for the first period (Figure 4a) and oscillating for the second (Figure 4b). The difference

between the SS and the data thus represent the detrended high frequency hydrologically driven fluctuations in stem radius and show a muted diel pattern during the period of rapid growth (Figure 4c) with the larger diel fluctuations during the second period indicating water limitation (Figure 4 d). The ZG model reveals only a single period of water deficit during the period of rapid growth (Figure 4e & g). During the period of limited growth, the ZG model shows two intervals of substantial growth (June 12th and June 13th - 14th), followed by an extended time of water deficit, reaching a maximum on June 14th and continuing until June 18th. Growth periods identified by the HMM are shown across all panels as vertical red stripes. During July, some growth was experienced on each day of the record, although this was minimal on July 19 following the only instanceof water deficit in this period. Following the ZG model, the HMM identified an interval of rapid growth beginning on June 13th and continuing to the early part of June 14th.

The distinct diel pattern observed during the two periods displayed in Figure 4 is also shown in the average response during a six-week window, centered on July 21st 2018, a period of time with active growth and fairly constant environmental conditions representative of the growing season (Figure 5). Sunrise during this period is detected by 7 am at our site, reaches a maximum of nearly 800 Wm^{-2} at noon and decreases more slowly in the afternoon (Figure 5a). Air temperatures follow a similar diel pattern reaching a minimum just before sunrise (mean of 19.6 °C). Temperatures build throughout the day reaching a maximum at 3:00 pm (mean of 24.9 °C), before decreasing again in the evening (Figure 5b). Finally, soil saturation shows a very distinct pattern related to the residential irrigation system used (Figure 5c). The system drip irrigates the plot just before sunrise thus reaching a maximum value regularly at 6 am for four days a week. The duration of irrigation is rather short (20 minutes), and thus by 7 am the saturation begins to drop with the rate of depletion accelerating as the sun comes up. At 11 am, a slight recovery occurs before soil water continues to be lower until the early evening, reaching a minimum at 4 pm. Averaging the instantaneous change in stem radius shows the same strong diel signal with the majority of stem swelling happening at night and stem shrinkage dominating the diurnal portion of the signal (Figure 5d). The similarities among the environmental conditions and the hydrologically driven fluctuations in stem radius can be seen by examining the residual to the smoothing spline. The diel pattern differs between the species as visible in the sinusoidal pattern of Spruce 1 (Figure 5e) or the more complex pattern of the cedar (Figure 5g). Both the pattern in the residuals and its derivative for Spruce 1 indicates that stem expansion is primarily at night. The maximum rate of stem shrinkage (the first derivative of the Spruce 1 residual) aligns with the average maximum air temperature (comparison of Figure 5b and Figure 5f). The trend displayed by the cedar is much less smooth than that of spruce but appears to correspond partially to diel fluctuations in soil saturation (Figure 5c).

Cold contraction events

Both spruce trees showed large stem contractions at temperatures at or below -5 °C (Figure 6), with prolonged exposure to these temperatures resulting in a greater magnitude of response. Stems did not appear to contract below freezing if the threshold of -5 °C was not reached. The cedar trees had no apparent stem response to cold temperatures.

CIT

We examined the statistical relationships between periods of growth and the ambient environmental conditions using machine learning to create conditional decision trees (Figure 7). This technique has the advantage that it not only partitions the growth response to local environmental conditions but also identifies specific values of these variables that can indicate a critical threshold of the response. Solar radiation, temperature, soil water content and VPD and precipitation were all found to be important, and distinct between the three trees (Figure 7). The rate of growth in Spruce 1 is significantly related to soil temperature with more growth happening when the soil is warmer than 17.5 °C. At cooler temperatures (below 17.5 °C), solar radiation becomes important with a critical value of 39.6 W m^{-2} splitting the response to two groups with higher growth rates with less light than with more light (Figure 7d). However, if soil temperatures were above 17.5 °C, a second critical temperature threshold is detected at 22.5 °C and growth is again higher above this temperature. Below either of the two temperature thresholds (17.5 or 22.5 °C) solar radiation appears as a significant variable and in both cases lower

light is associated with higher rates of growth. By comparison Spruce 2 and Cedar 1 were most responsive to variables related to water, namely VPD and precipitation (Figures 7e & 7f respectively). Precipitation edges out VPD for Spruce 2, with higher growth rates above 0.19 mm of rain than below. Below this threshold VPD is identified as a significant driver of growth with a critical threshold of 0.37 kPa. The importance of the two parameters is reversed for Cedar 1, yet the break points and the direction of the response are quite similar: VPD is the strongest predictor and has a threshold of 0.31 kPa while precipitation is secondary, splitting at 0.12 mm. The critical VPD value for the rate of growth is slightly higher than that for the amount of growth (0.23 vs. 0.31).

More differences in relevant environmental variables and their break points were found in the amount of growth using the decision tree approach, especially for the spruces (Figure 7a, b). Soil temperature takes the first position for Spruce 1 (threshold of 15 °C), followed by solar radiation (threshold of 55.6 W m^{-2}), and then soil water (threshold of 0.4 m^3 m^{-3}, Figure 7a). Overall this is a simpler set of values than was found significant for the rate of growth of this tree, yet the most complicated of three total growth relationships observed. By contrast Spruce 2 had the simplest decision tree, experiencing more growth when solar radiation was below 64.2 W m^{-2} than when it was above (Figure 7b). Finally, the variables identified as important to cedar growth are the same variables identified as important to the rate of growth in this tree: VPD (0.23 kPa) and precipitation (>0 mm) and show more growth occurs when the VPD is low and it is raining (Figure 7c).

Linear Models

We used multiple regression models to identify which combination of environmental variables had the most predictive power estimating growth (Table 2). The rate of growth for all trees was best explained by a model including air temperature, soil moisture, VPD and all of the interaction terms. No single environmental variable was significant on its own. This model explained growth (the amount of expansion during the growth periods) for the spruce trees, but not that of the cedar.

Discussion:

Dendrometers provide an accurate and precise record of short- (5 min) to long-term (annual) changes in stem diameter, giving a detailed signal of biological activity. This fine resolution allows comparison to environmental conditions that support growth from the hourly to yearly time scale. By streaming these data directly to the internet and adding co-located measurements of the environmental conditions, the system can provide highly useful, near real-time information and contribute to the "Internet of Nature" (Galle et al., 2019). This could allow homeowners or parks managers to optimize irrigation regimes to match watering to periods of rapid growth and/or water deficit (Ortuño et al., 2010), researchers to assess the impact of changing environmental conditions on carbon sequestration (Lada et al., 2019), and STEM educators to build lesson plans based on the scientific method and data collection for hypothesis testing (Sanders, 2012). Here we demonstrate many of these possibilities by monitoring trees in an urban setting. Our system identified the duration of the growing season, and within these periods can identify times of rapid growth and others when growth is limited by water availability. On finer time scales we show that growth (stem expansion) occurs primarily at night. Furthermore, simple models can help partition the dendrometer signal into hydraulics and growth components.

Seasonal growth trends:

Tracking the phenology and climatic response of trees in urban settings is critical to understanding both the ecosystem services urban trees provide and the effect changing environmental conditions are having on these services. Vegetation phenology, and particularly tree growth is often studied using remote sensing surveys of spectral reflectance (e.g. Ren et al., 2018), yet these studies can be challenging in urban settings due to the highly heterogeneous urban landscape and the relatively large spatial scales and infrequent flyover times of satellites (Melaas et al., 2016). Here we show that dendrometers can quantify both the short and long-term phenology of tree growth allowing urban arboriculturists to gain unique insights into the specific environmental conditions stimulating and retarding tree growth. In the urban setting studied, we find evergreen tree growth begins in late April and continues through the spring, summer, and fall, ending in late September (spruce) or

late October (cedar). The evergreen growth form of our study trees would have made this phenological timeline very difficult to detect without the real time dendrometer data and thus we suggest that networks of dendrometers in urban areas would provide a highly unique tool for arboriculturist to monitor growth and precisely time pruning, irrigation, and nutrient supply.

The onset of growth is likely triggered by warming temperatures (Begum et al., 2013), and changes in daylength (Oribe & Kubo, 1997; Chang et al., 2020). At our coastal location spruce growth is coincident with a daylength of 13hr, 20 min and an accumulated growing degree day of 69.7 °C. Despite being just twelve days behind, the initiation of radial expansion in the cedars is associated with longer days and much higher thermal accumulation (13hr, 45min and 160.6 °C). Experimental manipulations of *Cryptomeria* and *Larix* explored the possibility that bark thickness may affect the relative rate of warming and the breaking of cambial dormancy (Oribe & Kubo, 1997). As urban environments are typically warmer than their rural counterparts, they may have an earlier start to the growing season (Yang et al., 2020). While our study focused on a single suburban location, a monitoring system along an urban to rural gradient could provide additional insights into the links between urban environmental conditions and tree growth.

Detecting radial growth in evergreen trees can be difficult and may go unnoticed as it begins well in advance of leaf growth of the more common deciduous trees native to our study region and even the onset of leaf and stem elongation in these evergreen species (Oribe et al., 1993; as cited in Oribe & Kubo, 1997). Xylogenesis (the production of new xylem cells in the stems of trees) is linked to presence of indol-3-ylacetic acid (IAA) in the vascular cambium (Savidge & Wareing, 1981; Little & Savidge, 1987). This hormonal control may originate from degree day accumulation in buds and meristems, followed by IAA export to and presence in the cambium (Oribe & Kubo, 1997). Academic studies of *in situ* hormonal control of tree growth in urban settings are extremely rare, partially due to the difficulty of detecting cambial activity, but could be greatly facilitated with dendrometers, allowing for a more precise mechanistic understanding of urban tree growth. The simplicity and convenience of the automated dendrometer system can also provide homeowners, land managers and municipalities real-time information and the opportunity to initiate tree care when it will be most effective.

Radial growth continues throughout the spring summer and early fall and demonstrates a clear seasonal pattern, related to cold hardiness and surviving the winter (Catesson, 1994). Cold temperatures, a decreasing temperature trend, photoperiod, and changes in light quality (Chang et al., 2020) all cue the end of growth and cold hardening and are also altered by urbanization. During the late fall and winter seasons cell division stops, yet morphological (Wisniewski & Ashworth, 1986; Sagisaka et al., 1990; Kuroda & Sagisaka, 1993) and metabolic (Barnett, 1975; Sagisaka, 1981; Riding & Little, 1984; Kacperska, 1989; Catesson, 1990; Kuroda & Sagisaka, 1993) changes can still be observed and are considered essential for protection against freezing. After a brief resting phase when cell division is not possible, the cambium will remain in a quiescent stage (Catesson, 1994), capable of cell division once environmentally favorable conditions return. Dendrometers provide the opportunity to observe and even quantify these various stages of activity, creating unique learning and research opportunities. Placing dendrometers in urban settings enables study of how the built environment might alter the cold-response of trees and allows streaming data into classrooms and nature centers, providing a more proximate connection for urban residents to the natural world and support sustainable development (Kitchin, 2014; Galle et al., 2019).

The tracking of diameter growth provides the opportunity to study not only the onset and cessation of growth, but also the magnitude of carbon sequestration. The four small trees in our study gained a total of 45.4 kg of above ground dry mass, thereby sequestering 22.7 kg C, or 83.3 kg of CO_2 during the duration of the study (July 2018 August 2019, the time when the Spruce 1 sensor saturated) (Table 1). Adding 30% to conservatively account for changes in root mass, increases the amount of carbon sequestration to 29.5 kg of C or 108.3 kg of CO_2. Though an estimate, calculations like these, based on very precise data from point dendrometers in a variety of urban settings, would help refine our estimates of carbon storage provided by urban trees. This can be substantial: previous work by Nowak and Crane (2002), estimates that trees in New York City alone may store

as much as 1.2million tonnes of carbon, with an annual rate of net carbon sequestration of more than 20,000 tC yr^{-1}. Using a valuation of \$20.3 tC^{-1} (Fankhauser, 1994), Nowak and Crane (2002) estimated that the 700 million tonnes of carbon stored by urban trees in the US had a value of more than \$14 billion in 2001. As robust estimates of carbon storage and cycling become more important in light of climate change, land use change, and urbanization, networks of point dendrometers in urban settings can play an important role providing urban foresters and arboriculturist a reliable tool for monitoring and quantifying the urban contribution to biological carbon sequestration.

Intra-annual diameter fluctuations:
On time scales ranging from minutes to weeks, the patterns of expansion and contraction of tree stems provide a wealth of information related to tree biology useful to urban tree care professionals. Generally, when temperatures are above freezing and physiological activity has a clear influence on stem diameter, contraction is observed during the day as transpiration moves water through the stem more quickly than it can be replenished from the soils via the roots (Goldstein et al., 1998; Steppe & Lemeur, 2004; Köcher et al., 2013). At night, stems generally expand as transpiration slows to a minimum and the hydrologic balance tips towards the absorption of water from the soils and stem refilling, providing the turgor pressure necessary for cell expansion (Steppe et al., 2015). At our site more than 59% of all stem expansion happens at night when temperatures are lower, humidity is higher, the vapor pressure deficit is lower, and soil moisture is abundant (due to regular irrigation at this site) (figure 5d). The first derivative of the dendrometer signal illustrates the correspondence between the average solar cycle and stem diameter (as in Cocozza et al., 2009). These diel patterns in stem diameter provide a novel framework for the study of urban trees and forests and connect the observations to the underlying physiological processes that are themselves responding to environmental variation on similarly short-time scales. Understanding the links among the urban environment, tree biology and resultant ecosystem services will require the precise quantification of the relationships among these parameters.

Identifying stem growth:
To distinguish periods of growth from those of hydrologically driven fluctuations in stem radius, we used an existing model for partitioning the dendrometer data that "assumes zero growth during periods of stem shrinkage" (ZG model, Zweifel et al., 2016). This model limits its definition of growth to periods of time when new maximum stem radii are achieved and assumes stems cannot both shrink due to water deficit and grow due to cell expansion simultaneously (Zweifel, 2016; Zweifel et al., 2016). Non-growth periods under the ZG model can contain large fluctuations in recorded stem radius. These fluctuations are interpreted as either the loss of water from elastic tissues (shrinking stems) or refilling (swelling stems), as previous work has shown a very high fidelity between dendrometer stem radius measurements and tree water relations (Zweifel et al., 2005; Steppe et al., 2006; Zweifel et al., 2006). The ZG method defines these non-growth periods as Total Water Deficit (TWD): the difference between the preceding maximum stem radius and the measured stem radius, which is interpreted as the amount of water required to regain the maximum expanded state of the existing stem tissues (Zweifel et al., 2016). Mechanistic models for growth do exist but can be extremely complex and often require additional hard to collect physiological data (Zweifel et al., 2005; Deslauriers et al., 2007; De Schepper & Steppe, 2010; Sevanto et al., 2011; Zweifel et al., 2014; Chan et al., 2016; Mencuccini et al., 2017). Evidence for the lack of cell division and expansion during TWD does exist (Lockhart, 1965; Steppe et al., 2006; Zweifel, 2016; Zweifel et al., 2016) and thus we accept this logic for further analyses of stem fluctuations in an urban setting.

To identify distinct growth periods of the ZG model for further statistical analysis, we apply a Hidden Markov Model (HMM). Compared to the raw output of the ZG model, the HMM has the advantage of identifying blocks of time dominated by growth without requiring the dendrometer readings be monotonically increasing. This is based on the idea that even during a growth period, growth might not be observed between every five-minute increment. Rather than breaking up the growth period at every time step that does not show growth, the HMM labels growth periods based on changes in frequency of observed non-growth time steps and growth time steps. Fitting the HMM on the ZG model output allowed us to isolate distinct growth periods for use in

statistical analysis. Doing so helped us avoid autocorrelation that would result from treating ZG "growth" time steps independently. The ZG and HMM methods are shown for two six-day periods, one featuring rapid growth and the other showing a period of water limitation leading to obvious stem shrinkage (figure 4). On July 15th 2018, there appears to be a pause in growth (figure 4e), yet the trained HMM allows for estimated growth period to continue (shading shown as a vertical bar across figure 4a, c, e & g). Similar patterns can be seen on several other days in both six-day blocks. With measurements being collected so frequently by the dendrometers, the HMM provides an effective way to identify separate growth periods for comparing growth rates to average environmental conditions as discussed below.

Relationships between stem growth and local climatic conditions

White spruce is native to boreal forests (Abrahamson, 2015) *and thought to be commonly limited by both cool temperatures* (Achuff & La Roi, 1977) *and soil moisture* (McGuire et al., 2010). In our experiment, the conditional decision tree analysis for Spruce 1 identified low soil moisture and colder soil temperatures as retarding stem growth, yet previous studies have found that fluctuations in stem diameter are positively correlated with air (Ortuño et al., 2006; Devine & Harrington, 2011; Oberhuber et al., 2015; Dong et al., 2019), not soil temperatures. We suspect in our study, soil temperatures were buffered from short-term fluctuations in onshore winds and thus represent a more stable representation of the environmental temperature controlling growth of the stems inside these dense coniferous canopies. From the regression analysis, we conclude that spruce growth (the amount of expansion during the growth periods) is best explained by a model that contains information about air temperature, soil moisture, VPD and all of the interaction terms (Table 2). All of these variables are directly or indirectly related to environmental control of stem water status and have contributed to previous attempts to interpret dendrometer signals (Dong et al., 2019). However, while our best fit model can account for a significant amount of variation in the growth rate observations, it may have limited predictive capability as more than 70% of the variance is unaccounted for. The reason for this lack of predictive power is unclear but may indicate a need to include information on substrate availability or source/sink dynamics (Savidge, 1983, 1996, 2001; Dengler, 2001; Vaganov et al., 2011). Additional dendrometers spanning urban to rural ecosystems might enable further understanding of whether this decoupling from environmental conditions is a unique product of the urban environment.

We observed a similar pattern for cedar as described above for the spruce, yet the individual parameter estimates were quite different and indicate a stronger response to soil moisture and VPD. This difference may reflect the evolutionary history of this species. *Cryptomeria japonica* is an endemic monoecious conifer of Japan (Kimura et al., 2014) thought to have a distributional corresponding to moderate climatic conditions including annual precipitation of at least 1200 mm, annual temperature > 5.0 °C, (Tsukada, 1982; as cited by Kimura et al., 2014). In fact, the conditional decision trees suggest low VPDs are the strongest determinant of growth in this tree, with a critical threshold of 0.23 kPa (growth) and 0.31 kPa (growth rate). Observations of *Platycladus orientalis* stem dynamics similarly found a VPD threshold for radial growth (Dong et al., 2019). However, their study focused more specifically on stem shrinkage and thus found a much higher VPD threshold of 0.8 kPa (more shrinkage below than above this threshold) which they attributed to a stomatal response. Previous work on stem shrinkage suggests the response is to an interaction between soil water (the source for stem water) and VPD (the driving force for water loss *via* transpiration) (Garnier & Berger, 1986; Hinckley & Bruckerhoff, 1975; Grossiord et al., 2017) and is consistent with our findings here for the relationships with stem growth rather than stem shrinkage. In general, trees from the Cupressaceae are believed to drought tolerant, stemming from the evolution of drought-resistant xylem and a general increase in the carbon investment in xylem tissue (Pittermann et al., 2012), yet drought sensitive in the sense that tree rings of many members of this family faithfully record the occurrence of droughts (e.g. Sano et al., 2009; Buckley et al., 2017, 2018; B. Buckley pers. com.). Previous work on this species (Abe & Nakai, 1999; Abe et al., 2003), shows a detailed response of xylem development to stem water status suggesting both that the mechanism of response may be the same in our two species, and supporting a highly sensitive response in cedar. The experimental conditions used by Abe et al (2003) manipulated only soil irrigation and observed dramatic reductions in both cambial cell division and expansion, perhaps further suggesting this species is particularly susceptible to

changes in soil moisture. Just as with spruce, we had a greater capacity to account for variation in the rate of growth than in the amount of growth in cedar. Clearly our ability to predict short-term fluctuations in the rates and amounts of growth requires further study, particularly in the urban environment, and a more complete understanding of the physiological controls of cambial activity.

Cold contraction events.

We observed the growth of both species to end between September and November and thus winter is a period of relatively low activity. However, the dendrometers reveal interesting patterns related to cold temperatures that could have important implications for tree growth and survival (Krejza et al., 2020; Maruta et al., 2020). The stems of both spruce trees, but not the cedars, contracted rapidly when the temperature went below -5º C and rebounded just as quickly. Frost-induced reversible shrinkage has long been known to occur (Hoffmann, 1857; Sachs, 1860; both as cited in Zweifel & Häsler, 2000) and has experimentally been shown to emanate from the bark and other elastic tissues above the xylem, which can induce the exchange of water between the bark and the wood below (Zweifel & Häsler, 2000; Lintunen et al., 2017). Movement of water out of the xylem and into the bark causes the osmotic concentration of the xylem to increase, thereby preventing intracellular freezing (Loris et al., 1999). The -3 to -5°C "threshold" for contraction was similar to that shown previously for a variety of species in both experimental and field, though not urban, settings (Zweifel & Häsler, 2000; Cocozza et al., 2009; King et al., 2013; Charra-Vaskou et al., 2015; Charrier et al., 2017) and suggests physical control of both the response and the induction of frost tolerance in tree stems. The lack of such signals in the cedar trees is curious but maybe related to morphological characteristics of the stems (e.g. intercellular space between the xylem and bark, Niklas, 1992; Zweifel & Häsler, 2000; Améglio et al., 2001). A second possibility for the lack of response in cedar is a buffered response related to the thermal inertia of the wood caused by bark isolation, crown architecture or micro environmental conditions (Charrier et al., 2017). Despite the lack of active cell division and expansion during the winter months, dendrometers continue to provide important information regarding the stem response to environmental conditions that can be used to inform landowners and land managers about the growth potential and health of their trees in winter.

Conclusions and further opportunities.

We installed four, high-resolution point dendrometers in an urban setting and streamed the data to a project web page in near real time. The result was an unique two-year time series that provided deep insights into the growth of specimen trees growing in a residential area. From this time series were able to assess the phenology of stem growth and water deficits, the magnitude of growth and carbon sequestration, and the relationship between fluctuations in stem diameter and the ambient environmental conditions. We also introduce new analytical techniques, a hidden markov model and conditional decision trees, alongside established ones, smoothing splines, their residuals, and multiple linear regression models, to assist with the interpretation of the data. Overall, we suggest the decision tree technique is a useful way to search for important environmental variables and thresholds which can then be used to test more specific hypotheses related to the environmental control of stem growth and hydrology. Similarly, the HMM is a powerful tool for identifying periods of growth and dormancy that deserves further attention. From this unique data set and variety of statistical techniques we show that three modest ornamental trees sequestered 22.7 kg C, (or 83.3 kg of CO_2) Between July 2018 August 2019. We further demonstrate that the stem expansion is primarily a nocturnal phenomenon while stem shrinkage corresponds to the daylight hours. Although there were some important differences among our three trees, there are obvious general relationships with temperature, VPD and precipitation, suggesting water relations control growth. Finally, fascinating responses to cold temperatures were measured in the winter months. Detailed information like this is rare in urban environments and yet facilitates a deeper understanding of ecosystem dynamics that is useful to professionals involved in urban ecosystem management.

Dendrometers can be a power tool in urban settings and can provide deep insights for land owners and land managers in urban areas where trees provide important ecosystem services. With the data streaming to the web, in nearly real time, we suggest projects like ours can have tremendous outreach and educational potential. Fluctuations in stem diameter happening over remarkably short time scales and so clearly tied to the local

environmental conditions surprise people and bring tree biology to life. Sharing these data with the public at nature centers and during other outreach opportunities, or working with teachers in a K-12 educational setting, has always piqued curiosity and stimulated deeper thinking and inquiry in STEM topics. These real time data sets also provide an opportunity for teaching the scientific method, beginning with observation then generating hypotheses, data analysis, hypothesis testing and finally interpretation and the ability to begin the process again immediately, and with new information. Live-streaming tree growth data facilitates an even deeper understanding and appreciation of the biological activity of trees and the services they provide in urban environments and thus can be a powerful tool connecting urban social and ecological systems.

Literature cited

Abe H. & Nakai T. (1999) Effect of the water status within a tree on tracheid morphogenesis in *Cryptomeria japonica* D. Don. *Trees* **14:** 124–129

Abe H., Nakai T., Utsumi Y. & Kagawa A. (2003) Temporal water deficit and wood formation in *Cryptomeria japonica*. *Tree Physiology* **23:** 859–863

Abhijith K. V, Kumar P., Gallagher J., McNabola A., Baldauf R., Pilla F., Broderick B., Di Sabatino S. & Pulvirenti B. (2017) Air pollution abatement performances of green infrastructure in open road and built-up street canyon environments–A review. *Atmospheric Environment* **162:** 71–86

Abrahamson I. (2015) *Picea glauca*, white spruce. *Fire Effects Information System; US Department of Agriculture, Forest Service, Rocky Mountain Research Station, Fire Sciences Laboratory (Producer)*

Achuff P. L. & La Roi G. H. (1977) *Picea-Abies* forests in the highlands of northern Alberta. *Vegetatio* **33:** 127–146

Alonzo M., Bookhagen B. & Roberts D. A. (2014) Urban tree species mapping using hyperspectral and lidar data fusion. *Remote Sensing of Environment* **148:** 70–83

Améglio T., Cochard H. & Ewers F. W. (2001) Stem diameter variations and cold hardiness in walnut trees. *Journal of Experimental Botany* **52:** 2135–2142

Barnett J. R. (1975) Seasonal variation of organelle numbers in sections of fusiform cambium cells of *Pinus radiata* D. Don. *New Zealand Journal of Botany* **13:** 325–332

Begum S., Nakaba S., Yamagishi Y., Oribe Y. & Funada R. (2013) Regulation of cambial activity in relation to environmental conditions: understanding the role of temperature in wood formation of trees. *Physiologia Plantarum* **147:** 46–54

Bernhardt E. S., Band L. E., Walsh C. J. & Berke P. E. (2008) Understanding, managing, and minimizing urban impacts on surface water nitrogen loading. *Annals of the New York Academy of Sciences* **1134:** 61–96

Booth D. B. & Bledsoe B. P. (2009) Streams and urbanization. In: *The water environment of cities*, pp. 93–123. Springer.

Buckley B. M., Hansen K. G., Griffin K. L., Schmiege S., Oelkers R., D'Arrigo R. D., Stahle D. K., Davi N., Nguyen T. Q. T. & Le C. N. (2018) Blue intensity from a tropical conifer's annual rings for climate reconstruction: An ecophysiological perspective. *Dendrochronologia* **50:** 10–22

Buckley B. M., Stahle D. K., Luu H. T., Wang S.-Y. S., Nguyen T. Q. T., Thomas P., Le C. N. & Ton T. M. (2017) Central Vietnam climate over the past five centuries from cypress tree rings. *Climate Dynamics* **48:** 3707–3723

Calfapietra C., Fares S., Manes F., Morani A., Sgrigna G. & Loreto F. (2013) Role of Biogenic Volatile Organic Compounds (BVOC) emitted by urban trees on ozone concentration in cities: A review. *Environmental pollution* **183:** 71–80

Carreiro M. M., Howe K., Parkhurst D. F. & Pouyat R. V (1999) Variation in quality and decomposability of red oak leaf litter along an urban-rural gradient. *Biology and Fertility of Soils* **30:** 258–268

Catesson A.-M. (1994) Cambial ultrastructure and biochemistry: changes in relation to vascular tissue differentiation and the seasonal cycle. *International Journal of Plant Sciences* **155:** 251–261

Catesson A. M. (1990) Cambial cytology and biochemistry. [W:] The vascular cambium. Iqbal M.(red.).

Chameides W. L., Fehsenfeld F., Rodgers M. O., Cardelino C., Martinez J., Parrish D., Lonneman W., Lawson D. R., Rasmussen R. A. & Zimmerman P. (1992) Ozone precursor relationships in the ambient atmosphere. *Journal of Geophysical Research: Atmospheres* **97:** 6037–6055

Chan T., Hölttä T., Berninger F., Mäkinen H., Nöjd P., Mencuccini M. & Nikinmaa E. (2016) Separating water-potential induced swelling and shrinking from measured radial stem variations reveals a cambial growth and osmotic concentration signal. *Plant, Cell & Environment* **39:** 233–244

Chang C. Y., Bräutigam K., Hüner N. P. A. & Ensminger I. (2020) Champions of winter survival: cold acclimation and molecular regulation of cold hardiness in evergreen conifers. *New Phytologist*

Charra-Vaskou K., Charrier G., Badel E., Ponomarenko A., Bonhomme M., Mayr S. & Ameglio T. (2015) Dynamic of cavitation, embolism and water fluxes in trees during freeze-thaw cycle analysed by in vivo visualization. In: *Xylem International Meeting*, p. T19. INRA-Université de Bordeaux, Bordeaux (FRA).

Charrier G., Nolf M., Leitinger G., Charra-Vaskou K., Losso A., Tappeiner U., Améglio T. & Mayr S. (2017)

Monitoring of freezing dynamics in trees: a simple phase shift causes complexity. *Plant Physiology* **173:** 2196–2207

Cocozza C., Lasserre B., Giovannelli A., Castro G., Fragnelli G. & Tognetti R. (2009) Low temperature induces different cold sensitivity in two poplar clones (*Populus*× *canadensis* Mönch 'I-214'and *P. deltoides* Marsh.'Dvina'). *Journal of experimental botany* **60:** 3655–3664

Crawley M. J. (2012) *The R book*. John Wiley & Sons

Dengler N. G. (2001) Regulation of vascular development. *Journal of Plant Growth Regulation* **20:** 1–13

Denman E. C., May P. B. & Moore G. M. (2016) The potential role of urban forests in removing nutrients from stormwater. *Journal of environmental quality* **45:** 207–214

Deslauriers A., Anfodillo T., Rossi S. & Carraro V. (2007) Using simple causal modeling to understand how water and temperature affect daily stem radial variation in trees. *Tree Physiology* **27:** 1125–1136

Devine W. D. & Harrington C. A. (2011) Factors affecting diurnal stem contraction in young Douglas-fir. *Agricultural and Forest Meteorology* **151:** 414–419

Dochinger L. S. (1980) Interception of airborne particles by tree plantings. *Journal of environmental quality* **9:** 265–268

Dong M., Wang B., Jiang Y. & Ding X. (2019) Environmental Controls of Diurnal and Seasonal Variations in the Stem Radius of *Platycladus orientalis* in Northern China. *Forests* **10:** 784

Durbin R., Eddy S. R., Krogh A. & Mitchison G. (1998) *Biological sequence analysis: probabilistic models of proteins and nucleic acids*. Cambridge university press

Eddy S. R. (2004) What is a hidden Markov model? *Nature biotechnology* **22:** 1315–1316

Edmondson J. L., Davies Z. G., McHugh N., Gaston K. J. & Leake J. R. (2012) Organic carbon hidden in urban ecosystems. *Scientific reports* **2:** 963

Eitel J. U. H., Griffin K. L., Boelman N. T., Maguire A. J., Meddens A. J. H., Jensen J., Vierling L. A., Schmiege S. C. & Jennewein J. S. (2020) Remote sensing tracks daily radial wood growth of evergreen needleleaf trees. *Global Change Biology*

Elliott S. (2016) The potential for automating assisted natural regeneration of tropical forest ecosystems. *Biotropica* **48:** 825–833

Fankhauser S. (1994) The social costs of greenhouse gas emissions: an expected value approach. *The Energy Journal* **15:**

Galle N. J., Nitoslawski S. A. & Pilla F. (2019) The Internet of Nature: How taking nature online can shape urban ecosystems. *The Anthropocene Review* **6:** 279–287

Garnier E. & Berger A. (1986) Effect of water stress on stem diameter changes of peach trees growing in the field. *Journal of Applied Ecology***:** 193–209

Goldstein G., Andrade J. L., Meinzer F. C., Holbrook N. M., Cavelier J., Jackson P. & Celis A. (1998) Stem water storage and diurnal patterns of water use in tropical forest canopy trees. *Plant, Cell & Environment* **21:** 397–406

Grossiord C., Sevanto S., Borrego I., Chan A. M., Collins A. D., Dickman L. T., Hudson P. J., McBranch N., Michaletz S. T. & Pockman W. T. (2017) Tree water dynamics in a drying and warming world. *Plant, cell & environment* **40:** 1861–1873

Haase D. (2009) Effects of urbanization on the water balance–A long-term trajectory. *Environmental Impact Assessment Review* **29:** 211–219

Hamin E. M. & Gurran N. (2009) Urban form and climate change: Balancing adaptation and mitigation in the US and Australia. *Habitat international* **33:** 238–245

Harding R. B. & Grigal D. F. (1985) Individual tree biomass estimation equations for plantation-grown white spruce in northern Minnesota. *Canadian Journal of Forest Research* **15:** 738–739

Herrmann V., McMahon S. M., Detto M., Lutz J. A., Davies S. J., Chang-Yang C.-H. & Anderson-Teixeira K. J. (2016) Tree circumference dynamics in four forests characterized using automated dendrometer bands. *PloS one* **11:** e0169020

Himmelmann L. (2010) HMM: Hidden Markov Models. *R package version 1.0*

Hinckley T. M. & Bruckerhoff D. N. (1975) The effects of drought on water relations and stem shrinkage of *Quercus alba*. *Canadian Journal of Botany* **53:** 62–72

Hoffmann H. (1857) *Witterung und Wachsthum oder Grundzüge der Pflanzenklimatologie*. Förstner

Hothorn T., Hornik K. & Zeileis A. (2006) Unbiased Recursive Partitioning: A Conditional Inference Framework. *Journal of Computational and Graphical Statistics* **15:** 651–674

Hothorn T. & Zeileis A. (2015) {partykit}: A Modular Toolkit for Recursive Partitioning in {R} [WWW document]. *Journal of Machine Learning Research* **16:** 3905–3909 URL http://jmlr.org/papers/v16/hothorn15a.html

Idso C. D., Idso S. B. & Balling Jr R. C. (1998) The urban CO_2 dome of Phoenix, Arizona. *Physical Geography* **19:** 95–108

Ikin K., Knight E., Lindenmayer D. B., Fischer J. & Manning A. D. (2013) The influence of native versus exotic streetscape vegetation on the spatial distribution of birds in suburbs and reserves. *Diversity and Distributions* **19:** 294–306

Jenkins J. C., Chojnacky D. C., Heath L. S. & Birdsey R. A. (2003) National-scale biomass estimators for United States tree species. *Forest science* **49:** 12–35

Kacperska A. (1989) Metabolic consequences of low temperature stress in chilling-insensitive plants.

Kaushal S. S. & Belt K. T. (2012) The urban watershed continuum: evolving spatial and temporal dimensions. *Urban Ecosystems* **15:** 409–435

Ker M. F. & Raalte G. D. Van (1981) Tree biomass equations for *Abies balsamea* and *Picea glauca* in northwestern New Brunswick. *Canadian Journal of Forest Research* **11:** 13–17

Kimura M. K., Uchiyama K., Nakao K., Moriguchi Y., San Jose-Maldia L. & Tsumura Y. (2014) Evidence for cryptic northern refugia in the last glacial period in *Cryptomeria japonica*. *Annals of botany* **114:** 1687–1700

King G., Fonti P., Nievergelt D., Büntgen U. & Frank D. (2013) Climatic drivers of hourly to yearly tree radius variations along a 6 °C natural warming gradient. *Agricultural and Forest Meteorology* **168:** 36–46

Kitchin R. (2014) The real-time city? Big data and smart urbanism. *GeoJournal* **79:** 1–14

Köcher P., Horna V. & Leuschner C. (2013) Stem water storage in five coexisting temperate broad-leaved tree species: significance, temporal dynamics and dependence on tree functional traits. *Tree physiology* **33:** 817–832

Krejza J., Cienciala E., Světlík J., Bellan M., Noyer E., Horáček P., Štěpánek P. & Marek M. V (2020) Evidence of climate-induced stress of Norway spruce along elevation gradient preceding the current dieback in Central Europe. *Trees***:** 1–17

Kuroda H. & Sagisaka S. (1993) Ultrastructural changes in cortical cells of apple (*Malus pumila* Mill.) associated with cold hardiness. *Plant and cell physiology* **34:** 357–365

Lada H., Yen J. D. L., Cunningham S. C., Selwood K. E., Falcke P., Hodgson J. C. & Mac Nally R. (2019) Influence of climate on individual tree growth and carbon sequestration in native-tree plantings. *Austral Ecology* **44:** 859–867

Lintunen A., Lindfors L., Nikinmaa E. & Hölttä T. (2017) Xylem diameter changes during osmotic stress, desiccation and freezing in *Pinus sylvestris* and *Populus tremula*. *Tree physiology* **37:** 491–500

Little C. H. A. & Savidge R. A. (1987) The role of plant growth regulators in forest tree cambial growth. In: *Hormonal control of tree growth*, pp. 137–169. Springer.

Livesley S. J., McPherson E. G. & Calfapietra C. (2016) The urban forest and ecosystem services: impacts on urban water, heat, and pollution cycles at the tree, street, and city scale. *Journal of environmental quality* **45:** 119–124

Lockhart J. A. (1965) An analysis of irreversible plant cell elongation. *Journal of theoretical biology* **8:** 264–275

Loris K., Havranek W. M. & Wieser G. (1999) The ecological significance of thickness changes in stem, branches and twigs of Pinus cembra L. during winter. *PHYTON-HORN*- **39:** 117–122

Lovett G. M., Traynor M. M., Pouyat R. V, Carreiro M. M., Zhu W.-X. & Baxter J. W. (2000) Atmospheric deposition to oak forests along an urban− rural gradient. *Environmental science & technology* **34:** 4294–4300

Maruta E., Kubota M. & Ikeda T. (2020) Effects of xylem embolism on the winter survival of *Abies veitchii* shoots in an upper subalpine region of central Japan. *Scientific reports* **10:** 1–10

McGeehin M. A. & Mirabelli M. (2001) The potential impacts of climate variability and change on temperature-related morbidity and mortality in the United States. *Environmental health perspectives* **109:** 185–189

McGuire A. D., Ruess R. W., Lloyd A., Yarie J., Clein J. S. & Juday G. P. (2010) Vulnerability of white spruce tree growth in interior Alaska in response to climate variability: dendrochronological, demographic, and experimental perspectives. *Canadian Journal of Forest Research* **40:** 1197–1209

Melaas E. K., Wang J. A., Miller D. L. & Friedl M. A. (2016) Interactions between urban vegetation and surface urban heat islands: a case study in the Boston metropolitan region. *Environmental Research Letters* **11:** 54020

Mencuccini M., Salmon Y., Mitchell P., Hölttä T., Choat B., Meir P., O'grady A., Tissue D., Zweifel R. & Sevanto S. (2017) An empirical method that separates irreversible stem radial growth from bark water content changes in trees: theory and case studies. *Plant, cell & environment* **40:** 290–303

Niklas K. J. (1992) *Plant biomechanics: an engineering approach to plant form and function*. University of Chicago press

Nitoslawski S. A., Galle N. J., Van Den Bosch C. K. & Steenberg J. W. N. (2019) Smarter ecosystems for smarter cities? A review of trends, technologies, and turning points for smart urban forestry. *Sustainable Cities and Society* **51:** 101770

Norton B. A., Coutts A. M., Livesley S. J., Harris R. J., Hunter A. M. & Williams N. S. G. (2015) Planning for cooler cities: A framework to prioritize green infrastructure to mitigate high temperatures in urban landscapes. *Landscape and urban planning* **134:** 127–138

Nowak D. J., Bodine A. R., Hoehn R. E., Ellis A., Hirabayashi S., Coville R., Auyeung D. S. N., Sonti N. F., Hallett R. A. & Johnson M. L. (2018) The Urban Forest of New York City. Resource Bulletin NRS 117.

Nowak D. J. & Crane D. E. (2002) Carbon storage and sequestration by urban trees in the USA. *Environmental pollution* **116:** 381–389

Nowak D. J., Crane D. E. & Stevens J. C. (2006) Air pollution removal by urban trees and shrubs in the United States. *Urban forestry & urban greening* **4:** 115–123

Nrcs U. (2009) Web soil survey. *URL http://www. websoilsurvey. ncsc. usda. gov/app/[verified October 29, 2009]*

Oberhuber W., Kofler W., Schuster R. & Wieser G. (2015) Environmental effects on stem water deficit in co-occurring conifers exposed to soil dryness. *International journal of biometeorology* **59:** 417–426

Oribe Y. & Kubo T. (1997) Effect of heat on cambial reactivation during winter dormancy in evergreen and deciduous conifers. *Tree Physiology* **17:** 81–87

Oribe Y., Kubo T. & Fushitani M. (1993) Variations of cambial reactivation within stems in deciduous and evergreen conifers. *Bulletin of the Experiment Forests-Tokyo University of Agriculture and Technology (Japan)*

Ortuño M. F., Conejero W., Moreno F., Moriana A., Intrigliolo D. S., Biel C., Mellisho C. D., Pérez-Pastor A., Domingo R. & Ruiz-Sánchez M. C. (2010) Could trunk diameter sensors be used in woody crops for irrigation scheduling? A review of current knowledge and future perspectives. *Agricultural Water Management* **97:** 1–11

Ortuño M. F., García-Orellana Y., Conejero W., Ruiz-Sánchez M. C., Mounzer O., Alarcón J. J. & Torrecillas A. (2006) Relationships between climatic variables and sap flow, stem water potential and maximum daily trunk shrinkage in lemon trees. *Plant and Soil* **279:** 229–242

Palomino J., Muellerklein O. C. & Kelly M. (2017) A review of the emergent ecosystem of collaborative geospatial tools for addressing environmental challenges. *Computers, Environment and Urban Systems* **65:** 79–92

Pataki D. E., Alig R. J., Fung A. S., Golubiewski N. E., Kennedy C. A., McPherson E. G., Nowak D. J., Pouyat R. V & Romero Lankao P. (2006) Urban ecosystems and the North American carbon cycle. *Global Change Biology* **12:** 2092–2102

Pittermann J., Stuart S. A., Dawson T. E. & Moreau A. (2012) Cenozoic climate change shaped the evolutionary ecophysiology of the Cupressaceae conifers. *Proceedings of the National Academy of Sciences* **109:** 9647–9652

R Development Core Team (2006) R: A language and environment for statistical computing.
Ren Q., He C., Huang Q. & Zhou Y. (2018) Urbanization impacts on vegetation phenology in China. *Remote Sensing* **10:** 1905
Riding R. T. & Little C. H. A. (1984) Anatomy and histochemistry of *Abies balsamea* cambial zone cells during the onset and breaking of dormancy. *Canadian Journal of Botany* **62:** 2570–2579
Rudnicky J. L. & McDonnell M. J. (1989) Forty-eight years of canopy change in a hardwood-hemlock forest in New York City. *Bulletin of the Torrey Botanical Club***:** 52–64
Sachs J. (1860) Kristallbildung beim gefrieren und auftauen saftiger pflanzenteile, mitgeteilt von W. *Hofmeister. Ber Verh Sächs Akad Wiss* **12:** 1–50
Sagisaka S. (1981) Adenosine triphosphate levels in the poplar during one year of growth. *Plant and Cell Physiology* **22:** 1287–1292
Sagisaka S., Asada M. & Ahn Y. H. (1990) Ultrastructure of poplar cortical cells during the transition from growing to wintering stages and vice versa. *Trees* **4:** 120–127
Sanders M. E. (2012) Integrative STEM education as "best practice". In: Griffith Institute for Educational Research, Queensland, Australia.
Sano M., Buckley B. M. & Sweda T. (2009) Tree-ring based hydroclimate reconstruction over northern Vietnam from *Fokienia hodginsii*: eighteenth century mega-drought and tropical Pacific influence. *Climate dynamics* **33:** 331
Sarda-Espinosa A., Subbiah S. & Bartz-Beielstein T. (2017) Conditional inference trees for knowledge extraction from motor health condition data. *Engineering Applications of Artificial Intelligence* **62:** 26–37
Savidge R. (2001) Intrinsic regulation of cambial growth. *Journal of Plant Growth Regulation* **20:** 52–77
Savidge R. A. (1983) The role of plant hormones in higher plant cellular differentiation. II. Experiments with the vascular cambium, and sclereid and tracheid differentiation in the pine, *Pinus contorta*. *The Histochemical journal* **15:** 447–466
Savidge R. A. (1996) Xylogenesis, genetic and environmental regulation-a review. *Iawa Journal* **17:** 269–310
Savidge R. A. & Wareing P. F. (1981) Plant growth regulators and the differentiation of vascular elements. *Xylem cell development***:** 192–235
De Schepper V. & Steppe K. (2010) Development and verification of a water and sugar transport model using measured stem diameter variations. *Journal of experimental botany* **61:** 2083–2099
Sevanto S., Hölttä T. & Holbrook N. M. (2011) Effects of the hydraulic coupling between xylem and phloem on diurnal phloem diameter variation. *Plant, Cell & Environment* **34:** 690–703
Shepherd J. M., Pierce H. & Negri A. J. (2002) Rainfall modification by major urban areas: Observations from spaceborne rain radar on the TRMM satellite. *Journal of applied meteorology* **41:** 689–701
Solecki W. D., Rosenzweig C., Parshall L., Pope G., Clark M., Cox J. & Wiencke M. (2005) Mitigation of the heat island effect in urban New Jersey. *Global Environmental Change Part B: Environmental Hazards* **6:** 39–49
Sonti N. F., Hallett R. A., Griffin K. L. & Sullivan J. H. (2019) White oak and red maple tree ring analysis reveals enhanced productivity in urban forest patches. *Forest Ecology and Management* **453:** 117626
Spurr S. H. & Brown Jr C. T. (1946) Specifications for aerial photographs used in forest management. *Photogrammetric Engineering* **12:** 131–141
Steinberg D. A., Pouyat R. V, Parmelee R. W. & Groffman P. M. (1997) Earthworm abundance and nitrogen mineralization rates along an urban-rural land use gradient. *Soil Biology and Biochemistry* **29:** 427–430
Steppe K. & Lemeur R. (2004) An experimental system for analysis of the dynamic sap-flow characteristics in young trees: results of a beech tree. *Functional Plant Biology* **31:** 83–92
Steppe K., De Pauw D. J. W., Lemeur R. & Vanrolleghem P. A. (2006) A mathematical model linking tree sap flow dynamics to daily stem diameter fluctuations and radial stem growth. *Tree physiology* **26:** 257–273
Steppe K., Sterck F. & Deslauriers A. (2015) Diel growth dynamics in tree stems: linking anatomy and ecophysiology. *Trends in plant science* **20:** 335–343
Thomas S. C. & Martin A. R. (2012) Carbon content of tree tissues: a synthesis. *Forests* **3:** 332–352
Tsukada M. (1982) *Cryptomeria japonica*: Glacial refugia and late-glacial and postglacial migration. *Ecology* **63:** 1091–1105

Vaganov E. A., Anchukaitis K. J. & Evans M. N. (2011) How well understood are the processes that create dendroclimatic records? A mechanistic model of the climatic control on conifer tree-ring growth dynamics. In: *Dendroclimatology*, pp. 37–75. Springer.

Walsh C. J., Fletcher T. D. & Burns M. J. (2012) Urban stormwater runoff: a new class of environmental flow problem. *PLOS one* **7:** e45814

Weng Q. (2003) Fractal analysis of satellite-detected urban heat island effect. *Photogrammetric engineering & remote sensing* **69:** 555–566

Wisniewski M. & Ashworth E. N. (1986) Seasonal variation in deep supercooling and dehydrative resistance. *HortScience* **21:** 503–505

Yang J., Luo X., Jin C., Xiao X. & Xia J. C. (2020) Spatiotemporal patterns of vegetation phenology along the urban–rural gradient in Coastal Dalian, China. *Urban Forestry & Urban Greening* **54:** 126784

Zhu W.-X. & Carreiro M. M. (2004) Variations of soluble organic nitrogen and microbial nitrogen in deciduous forest soils along an urban–rural gradient. *Soil Biology and Biochemistry* **36:** 279–288

Zweifel R. (2016) Radial stem variations–a source of tree physiological information not fully exploited yet. *Plant, Cell & Environment* **39:** 231–232

Zweifel R., Drew D. M., Schweingruber F. & Downes G. M. (2014) Xylem as the main origin of stem radius changes in Eucalyptus. *Functional Plant Biology* **41:** 520–534

Zweifel R., Haeni M., Buchmann N. & Eugster W. (2016) Are trees able to grow in periods of stem shrinkage? *New Phytologist* **211:** 839–849

Zweifel R. & Häsler R. (2000) Frost-induced reversible shrinkage of bark of mature subalpine conifers. *Agricultural and forest meteorology* **102:** 213–222

Zweifel R., Zimmermann L. & Newbery D. M. (2005) Modeling tree water deficit from microclimate: an approach to quantifying drought stress. *Tree physiology* **25:** 147–156

Zweifel R., Zimmermann L., Zeugin F. & Newbery D. M. (2006) Intra-annual radial growth and water relations of trees: implications towards a growth mechanism. *Journal of experimental botany* **57:** 1445–1459

Tables:

Table 1. Characteristics of the four study trees, including Diameter at Breast Height (DBH), Basal Area Increment (BAI), and biomass. Above ground biomass (AGB) estimated using allometric equations. Below ground Biomass estimated as 30% of AGB, see text for more details. *Note:* Cedar 2 did not grow during the first season and was not included in further analysis.

			Above Ground Biomass			Below Ground Biomass		
	DBH (cm)	BAI (m2)	Initial (kg)	Final (kg)	Gain (kg)	Initial (kg)	Final (kg)	Gain (kg)
Spruce 1	11.5	37.2	33.3	48.4	15.1	8.2	11.4	3.1
Spruce 2	14.0	29.0	54.5	70.5	16.0	12.6	15.7	3.1
Cedar 1	16.7	17.3	77.0	91.3	14.4	18.0	21.1	3.1
Cedar 2	16.1	—	—	—	—	—	—	—
Total		83.50	164.81	210.19	45.39	38.83	48.07	9.25
Mean		27.83	54.94	70.06	15.13	12.94	16.02	3.08
SEM		5.774	12.596	12.395	0.471	2.827	2.805	0.025

Table 2: AIC selected models for linear regressions for the slope and growth of Spruce 1, Spruce 2, and Cedar 1 against environmental variables. Each tree has a single model which includes all three environmental variables and their interactions. AirT = air temperature (°C), soilsat = soil saturation (mS cm^{-1}), VPD = vapor pressure deficit (kPa), coef = coefficient, SE = standard error.

Summary of AIC selected models of linear regressions for nighttime growth versus environmental variables

		air temperature		soil saturation		VPD		airT:soilsat		airT:VPD		soilsat:VPD		airT:soilsat:VPD		model adj R^2
		coef	SE	coef	SE	coef	SE	coef	SE	coef	SE	coef	SE	coef	SE	
Spruce 1	ln(slope)	0.40	0.27	6.67	5.53	69.40	30.59	-0.30	0.29	-3.88	1.79	-70.96	32.60	3.80	1.92	0.27 *
	ln(growth)	-0.25	0.20	-6.29	4.01	-1.00	0.55	0.31	0.22	----	----	----	----	----	----	0.05 *
Spruce 2	ln(slope)	0.24	0.18	4.19	3.48	49.71	33.17	-0.32	0.19	-3.11	1.75	-37.67	36.47	2.37	1.87	0.28 *
	ln(growth)	0.35 *	0.15 *	3.17	2.91	-2.20 *	0.89 *	-0.36 *	0.16 *	----	----	----	----	----	----	0.13 *
Cedar 1	ln(slope)	0.25	0.69	11.36	16.45	153.39	89.98	-0.25	0.81	-6.11	5.25	-156.25	105.17	5.86	6.17	0.19 *
	ln(growth)	-0.13	0.45	-2.80	10.03	-0.46	1.80	0.16	0.52	----	----	----	----	----	----	-0.10

*p<0.05

Figure Legends:

Figure 1. Conceptual overview of the environmental drivers of urban tree growth and resulting ecosystem services provided by suburban trees considered when monitoring tree growth with point-dendrometers. A) Experimental protocol relies on point dendrometers attached to tree stems at 1.37 m from the ground. Also shown are the all-in-one weather station, soil temperature and moisture sensor and cell phone enabled data logger. Urban trees provide a variety of ecosystem services including: local cooling, carbon sequestration, removal of air pollutants, reduced erosion and runoff, and improved nutrient cycling. B) A dendrometer is mounted to the heartwood and holds the sensors in contact with the bark. The measurement detects changes in the elastic tissues below including the bark, phloem, cambium, and immature xylem. C) a photograph of one of the study trees highlighting the installed dendrometer.

Figure 2. Weather conditions over the two-year period of the study (2018 to 2019). Solar radiation (orange) (W m^{-2}) and precipitation (blue)(mm) make up the top panel. Maximum daily soil temperature (black) and air temperature (red) (℃) are in the second panel, and Volumetric Soil Water Content in the third (mm mm^{-3}).

Figure 3. Tree Growth, measured as linear distance (cm) from June 03 2018 until November 11 2019. Replicate trees of spruce (*Picea glauca*) and cedar (*Cryptomeria japonica*) are shown. The initial tree diameter (cm) at the height of the sensors is shown. Dotted vertical lines show the calculated end of the 2018 growing season, start of the 2019 growing season, and end of the 2019 growing season (cedar only). The end of the 2019 spruce signal is related to reaching the maximum sensor displacement. during the winter show periods of rapid stem contraction (see text). Lines highlighted in grey indicated loss of 25% or more of daily data as a result of battery life. Cedar 2, while visibly healthy, grew very little during the experimental period. Red circles show freezing temperature excursions for Spruce 1 and Spruce 2.

Figure 4. Radial growth over two, one-week time periods, one with a hydrated stem (7/14/18 to 7/20/18) and one experiencing dehydration (6/12/19 to 6/18/19) with multiple models applied to each. Panels a and b compare the spline to delta stem radius, a is a period of rapid growth, and b contains both periods of growth and periods of water deficit. Panels c and d show the residuals of the smoothing spline in each respective period. Figures e and f show the zero growth model and g and h show the total water deficit. The red vertical stripes indicate HMM identified growth periods.

Figure 5. Hourly average observations during the three weeks before and three weeks after July 21st. Panel a-c: environmental data in panels a b and c (solar radiation, Air temperature, and Soil saturation respectively). Panel d: boxplot of the hourly average change in the stem radius. Panel e & f, Spruce 1 spline residuals and derivative of the residuals. Panel f: Cedar spline residuals. Note data points showing no change were not included, and statistical outliers were discarded to emphasize the magnitude of change occurring.

Figure 6. Response of stem radius to cold winter temperatures. Red dashed lines connote temperatures of -5 ℃ and below. Intensity of the red hue is representative of the duration of the cold temperatures.

Figure 7. CITs partitioning the influence of environmental variables on total amount of log(growth) during HMM-identified growth periods (a-c) and on log(slope) across HMM-identified growth periods (d-f), calculated using values of the zero-growth model at the beginning and end points of each growth period. a) Spruce 1, growth. Soil temp was the most important predictor, and solar and soil water were also identified as influential. b) Spruce 2, growth. Solar was identified as the most important predictor. c) Cedar 1, growth. VPD was the most important predictor, and precip was also identified as influential. d) Spruce 1, slope. Soil temp was the most important predictor, but solar was also identified as influential. e) Spruce 2, slope. Precip was identified as the most important predictor, with VPD also identified as influential. f) Cedar 1, slope. VPD was the most important predictor, and precip was also influential.

Figure 1.

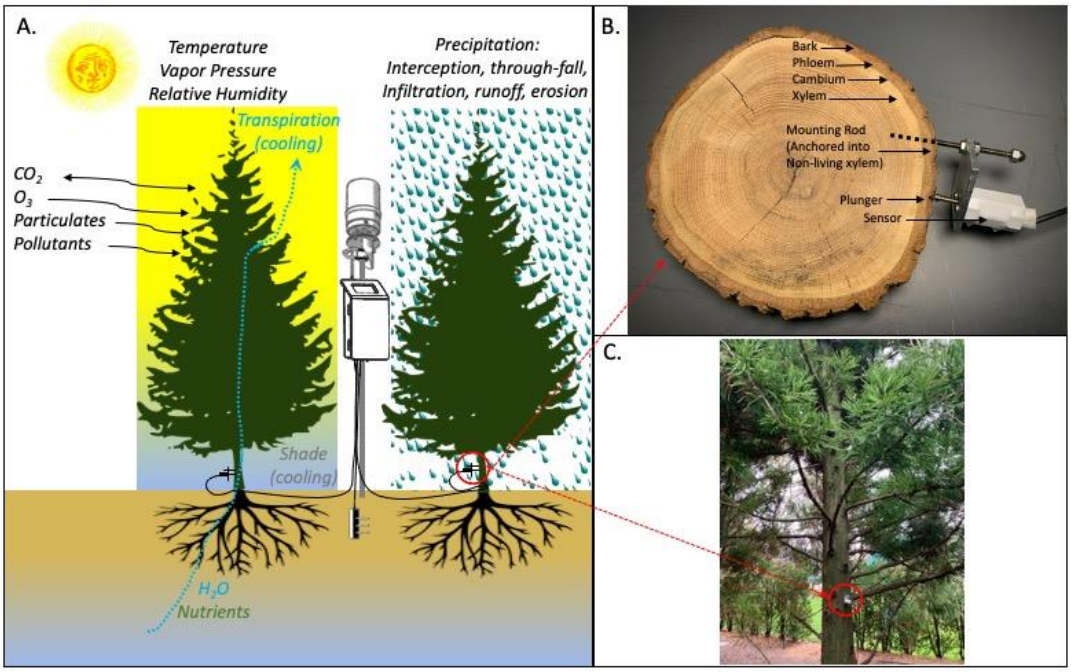

Figure 2.

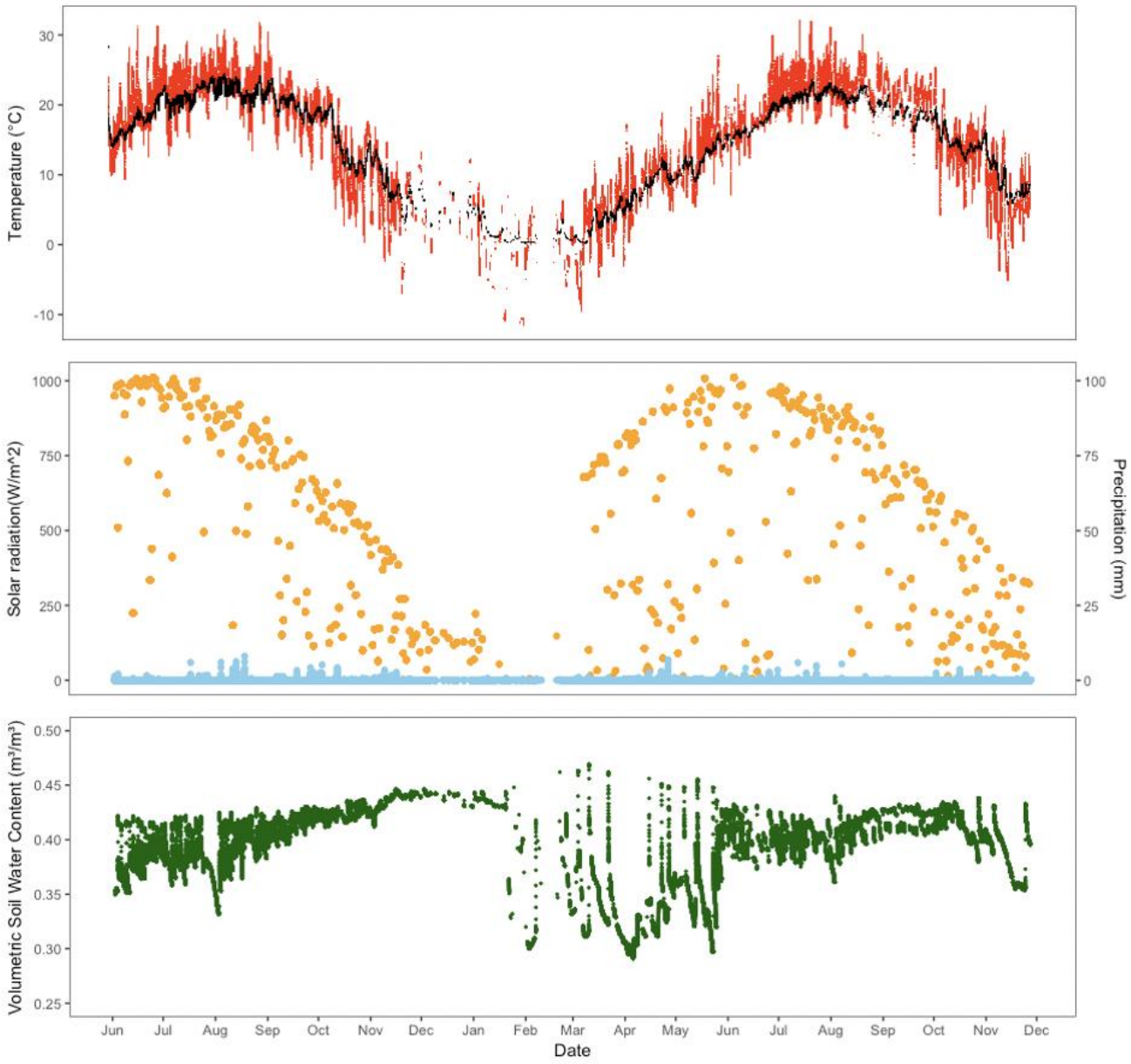

Figure 3.

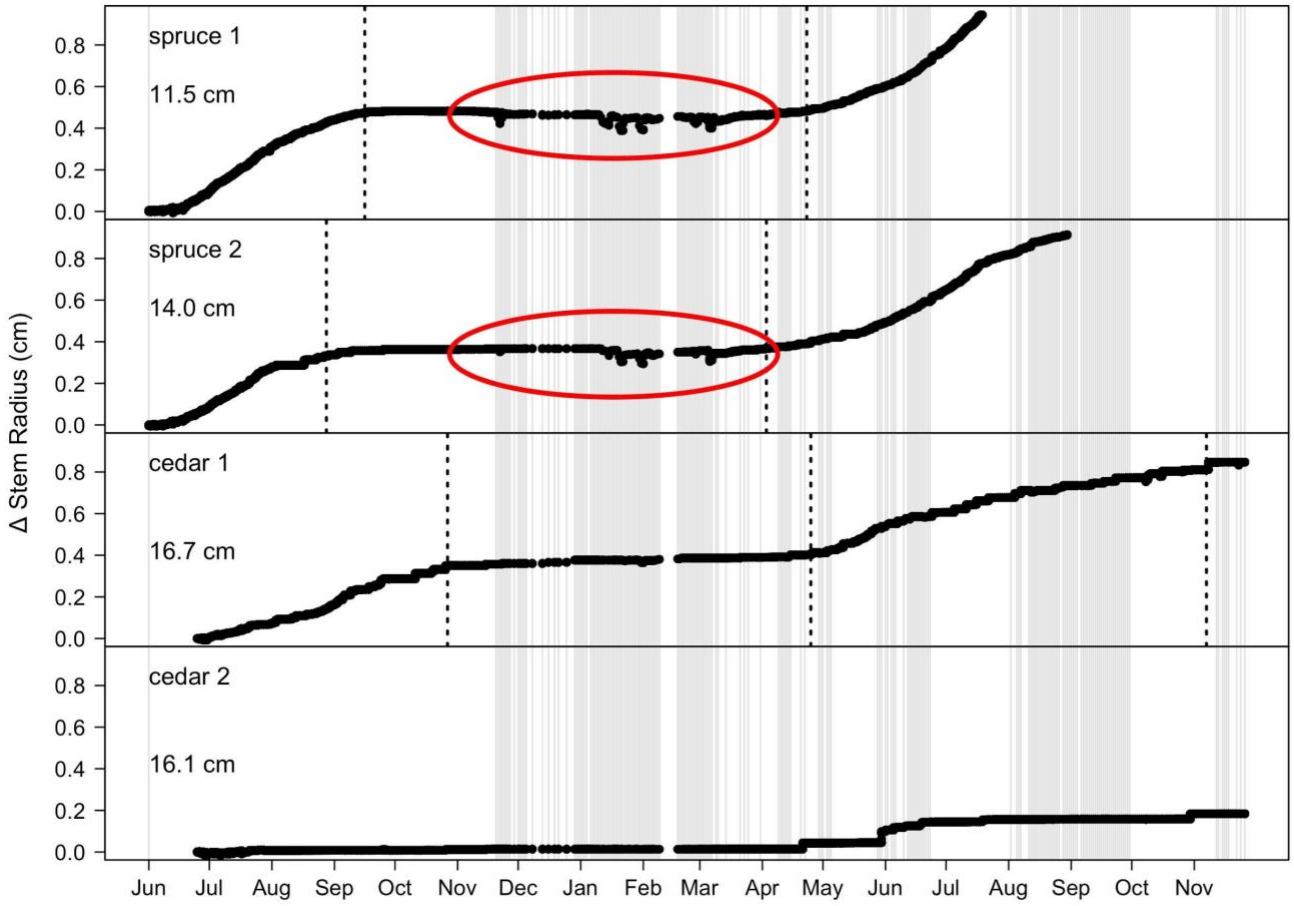

Figure 4.

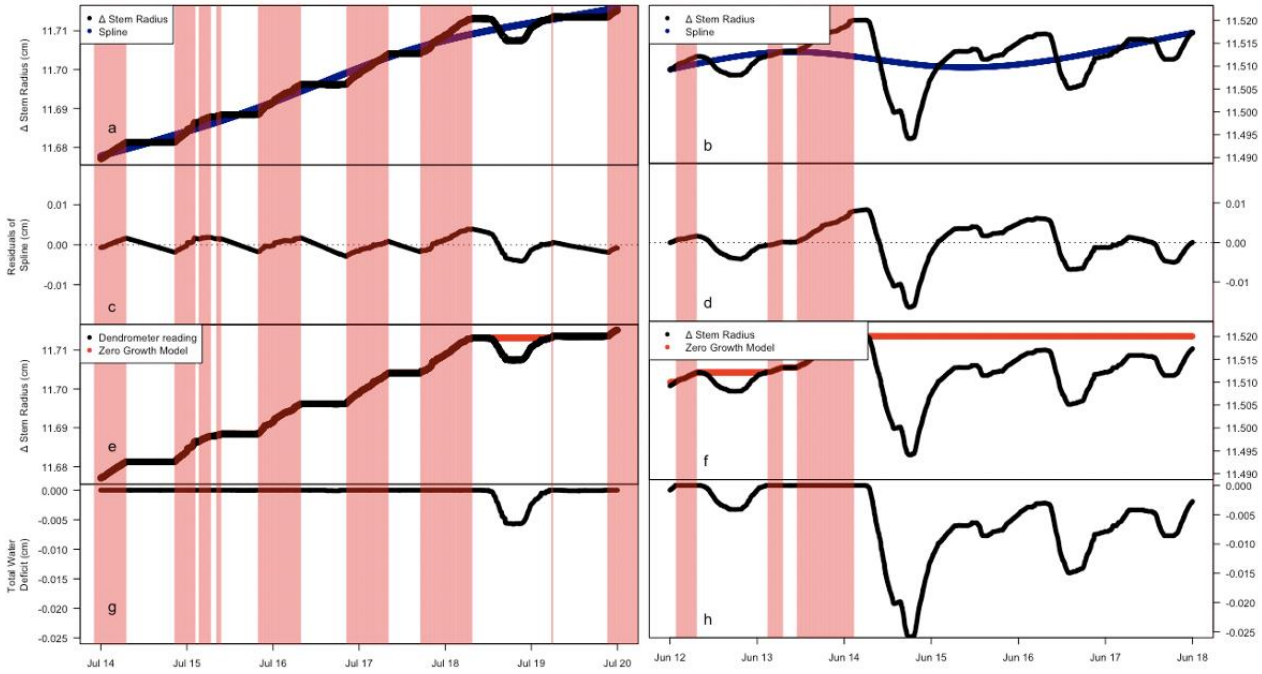

Figure 5.

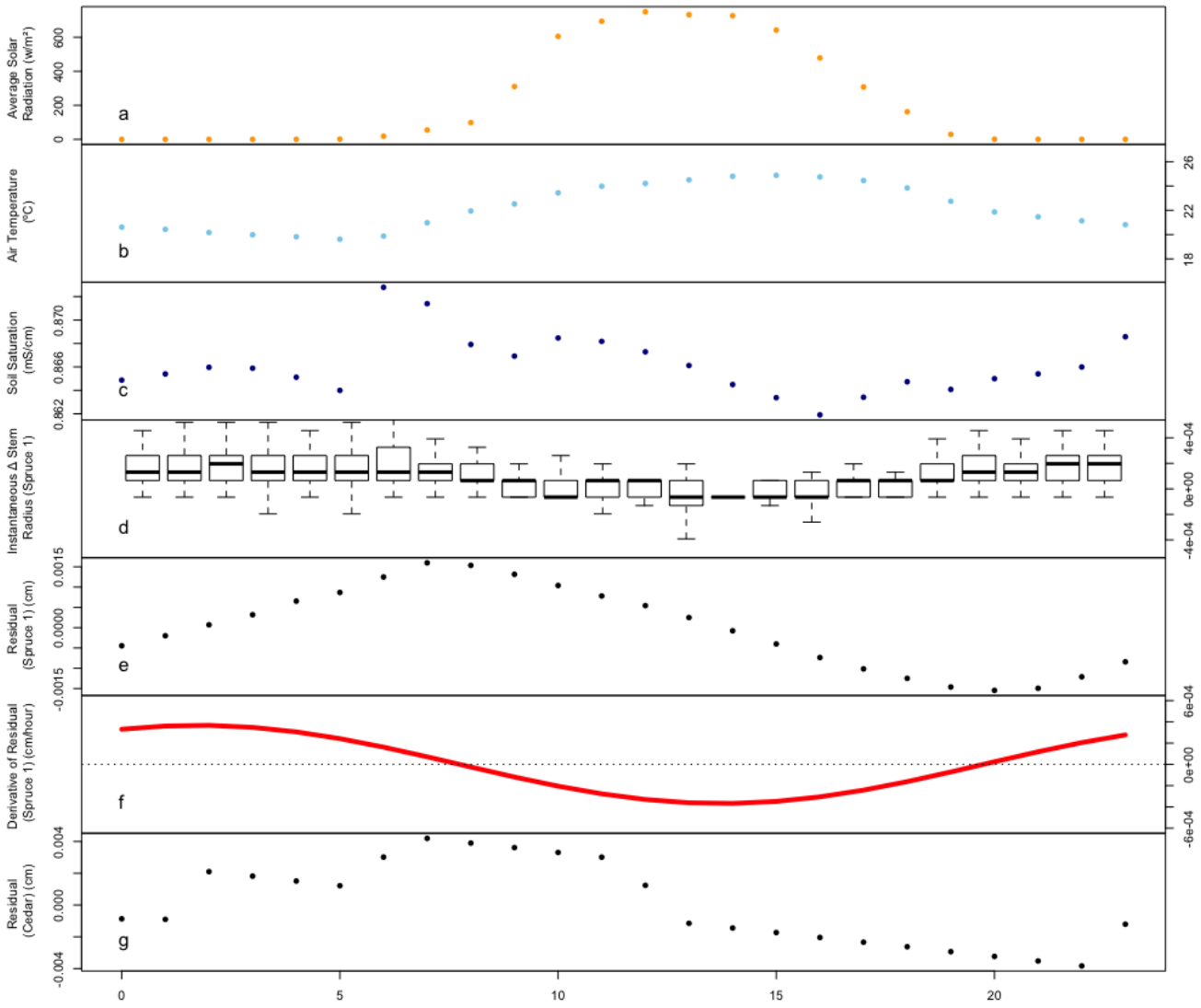

Figure 6.

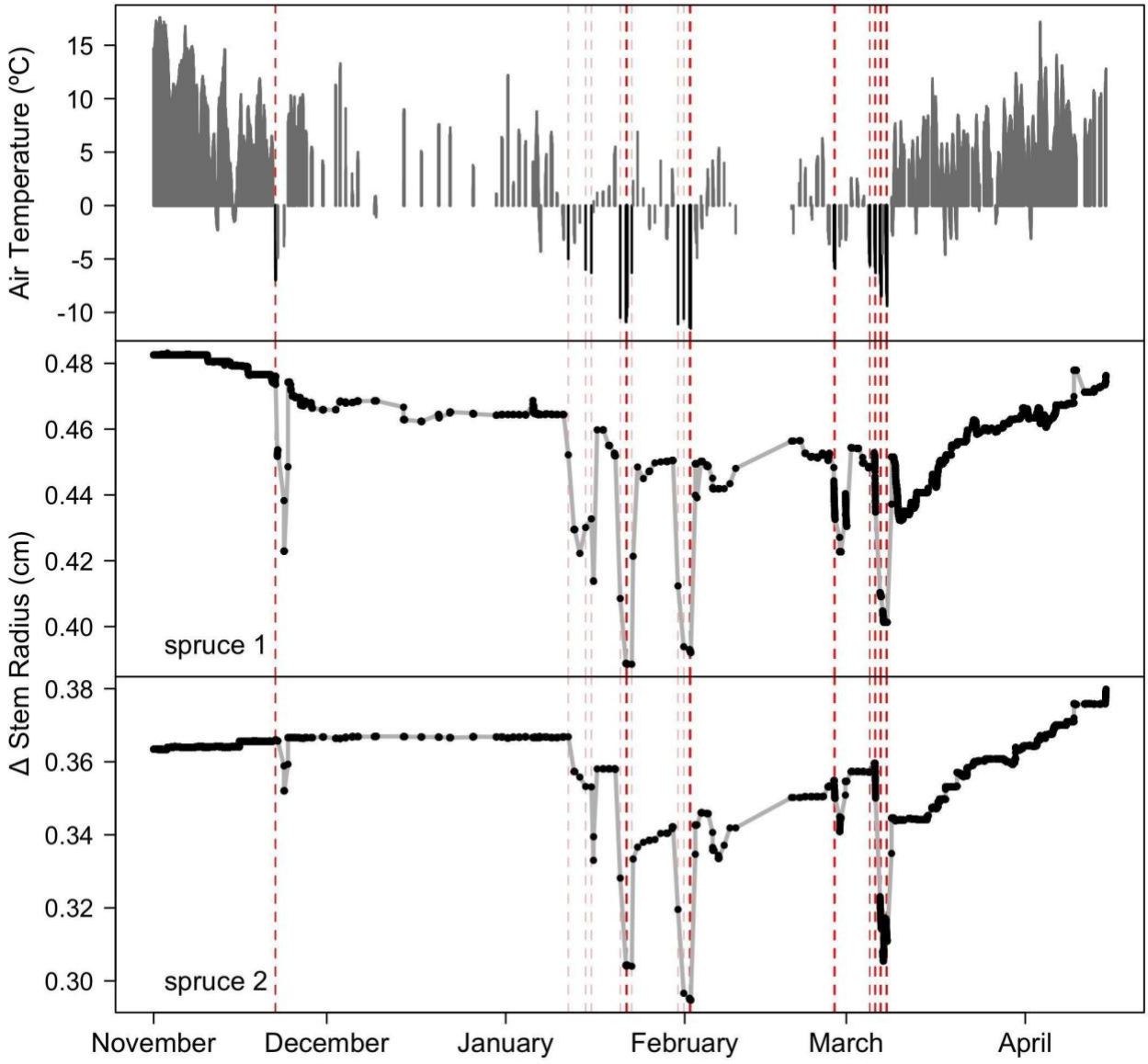

Figure 7.